53

SATELLITE & MESOMETEOROLOGY
RESEARCH PROJECT

Department of the Geophysical Sciences
The University of Chicago

ESTIMATED WIND SPEEDS OF THE PALM SUNDAY TORNADOES

by

Tetsuya Fujita

(Chapter VII of a Comprehensive Study of the Palm Sunday Tornadoes, 1965)

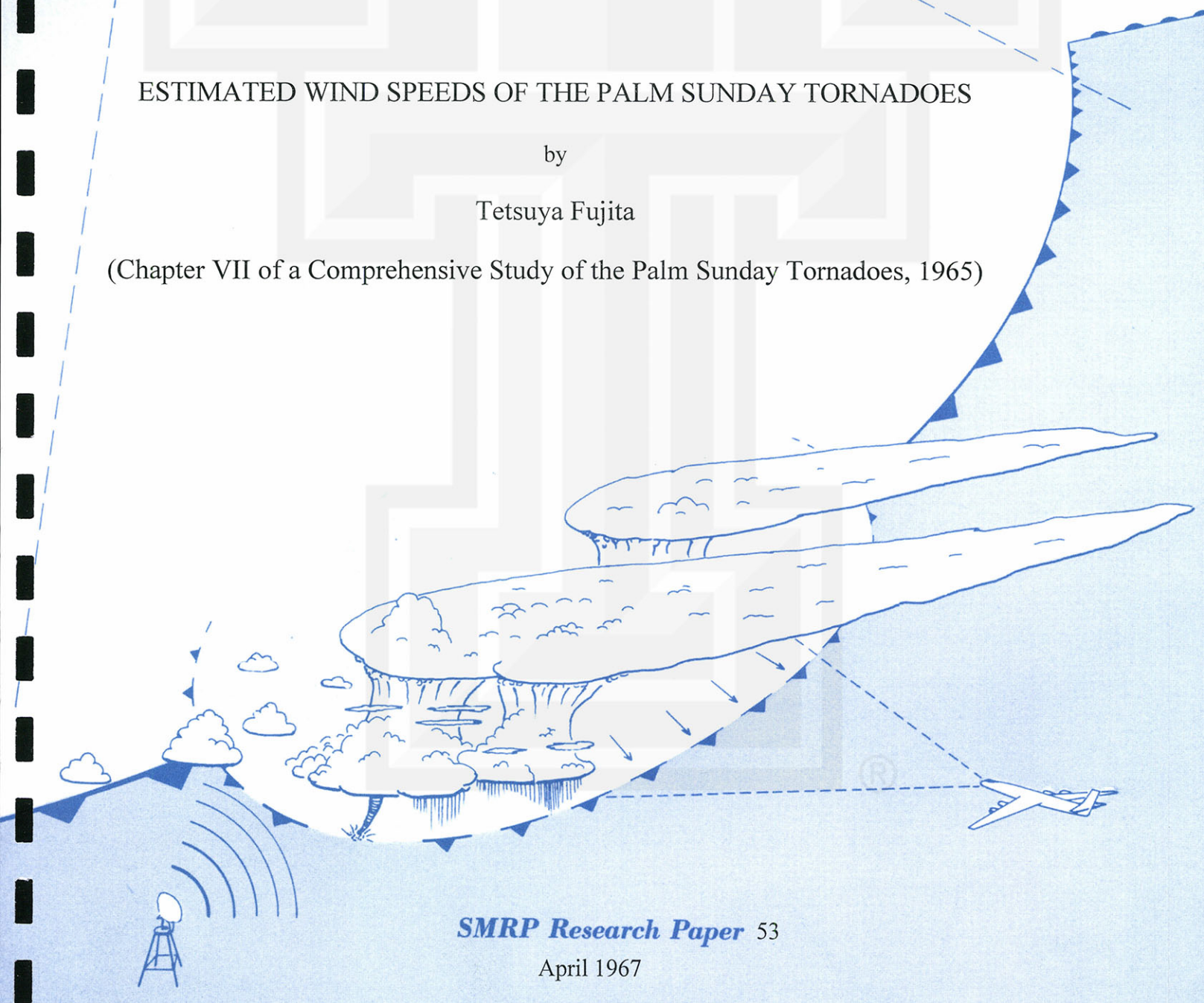

SMRP Research Paper 53

April 1967

SATELLITE AND MESOMETEOROLOGY RESEARCH PROJECT
Department of the Geophysical Sciences
The University of Chicago

ESTIMATED WIND SPEEDS OF THE PALM SUNDAY TORNADOES

by
Tetsuya Fujita

(Chapter VII of a Comprehensive Study of the Palm Sunday Tornadoes, 1965)

SMRP Research Paper #53
April 1967

The research presented in this paper has been sponsored by the U.S. Environmental Science Services Administration under grant No. E-86-67-(G).

ESTIMATED WIND SPEEDS OF THE PALM SUNDAY TORNADOES[1]

Tetsuya Fujita

Department of the Geophysical Sciences

The University of Chicago

Chicago, Illinois

ABSTRACT

The wind speed of a tornado in relation to its parent tornado cyclone is discussed in this last chapter[2] on the Palm Sunday tornadoes. One of the most interesting wind traces in this study, obtained from Tecumseh, Michigan, showed a peak gust speed of 151 mph, at which time the recorder pen went off the scale. The radial distribution of gust speeds around the tornado indicated that the outer vortex of the tornado was characterized by an irrotational wind field in which the product of v and r is constant. An indirect wind-speed estimate was attempted by examining the characteristic cycloidal marks left on the fields along the tornado paths. These marks are assumed to be produced by several spots rotating with the tornado funnel. Micro-scale convergence effects beneath these spots are estimated to be much larger than in other parts of the funnel, so that streaks of disturbed features remain along the cycloidal paths of these spots. The computed tangential speed of the spots is slightly higher than 100 mph inside the tornado paths of moderate damage.

---

[1] The research presented in this paper has been sponsored by the U.S. Environmental Science Services Administration under grant No. E-86-67-(G).

[2] A comprehensive study of the Palm Sunday tornadoes of April 11, 1965 was originally planned to include the following seven chapters:

Chapter I - Locations and Times of Tornadoes,

Chapter II - Aerial Survey of the Palm Sunday Tornadoes. SMRP Rep. No. 49,

Chapter III - The Synoptic Situation,

Chapter IV - Early Stage of Tornado Development as Revealed by Satellite Photographs. SMRP Rep. No. 50,

Chapter V - Features and Motions of Radar Echoes. SMRP Rep. No. 51,

Chapter VI - Stability and Differential Advection Associated with Tornado Development. SMRP Rep. No. 52,

Chapter VII - Estimated Wind Speeds of the Palm Sunday Tornadoes. SMRP Rep. No. 53.

Chapter VII concludes the portion to be submitted by SMRP. Further plans for the completion and publication of the comprehensive study are being considered.

1. Introduction

The Palm Sunday tornadoes had many remarkable features. Due to the rapid motion of the parent thunderstorms, most of the tornadoes traveled at a rate in excess of 60 mph. One by one, as many as six tornadoes were systematically born out of the parent thunderstorm as described in Chapter V (SMRP Research Paper No. 51). Moreover, a rare event occurred when one of the tornadoes passed a short distance from a wind recorder which indicated a 151 mph gust. Since most of these tornadoes occurred within a few hundred miles of Chicago, an easy flying distance, a large number of aerial photographs were obtained for the purpose of examining the damage areas which might include features related to the speed of the tornadic winds.

Even though this study does not conclusively establish the wind speed of tornadoes, the discussion presented will stimulate interest on tornado winds among those who wish to investigate the nature of the most violent vortex in the atmosphere.

2. Recorded Traces of Tornado and Tornado Cyclone Winds

Despite the fact that the Palm Sunday tornadoes of April 11, 1965 left more than 30 damage paths over a six-state area, only one anemometer was near enough to a path to record tornado-related winds. This one was located at Meyers Airport, north of Tecumseh, Michigan and was operated by the Tecumseh Community Health Study, the University of Michigan. As indicated in aerial survey map No. 11 in Chapter II (Fig. 13, SMRP Research Paper No. 49), the wind tower was located along the southern boundary of a very wide damage path resulting mainly from tornado J-4. The anemometer recorded a peak gust of 151 mph at 1907 CST. About one hour later another tornado, K-3, passed north of the same anemometer, recording a 75 mph peak gust at 2004 CST. The gust recorder trace converted into rectangular coordinates with wind direction added is shown in Fig. 1. It is seen that the wind speed increased from about 30 mph to 151 mph in about 15 min, then dropped back to 30 mph in three to four minutes. After the passage of the first tornado, J-4, the wind direction returned to southerly and remained there until about 10 min before the arrival of the second storm, K-3. The latter was located just ahead of the cold front, referred to as a dry cold front in previous chapters. Note that a straight westerly wind with a gust up to 70 mph came shortly after this storm.

According to the analysis of the radar echoes as presented in Figs. 17 and 18 in Chapter V (SMRP Research Report No. 51) these two tornadoes were born

from two separate thunderstorms which traveled along almost identical paths. A reduced gain picture of these thunderstorms taken by the Detroit (DTW) WSR-57 radar at 1852 CST appears in Fig. 2. Both echoes show distinct hook with a cyclonic finger located in the southwest quadrant.

3. Review of the Formation of Vault and Eye in a Rotating Thunderstorm

It has been well documented that tornadoes appear in the vicinity of a hook echo characterized by a well-defined finger or a 6-shaped configuration observed in the southwest quadrant of a thunderstorm echo obtained by low-level, reduced-gain PPI scans. In Browning's and Fujita's (1965) comments and reply on the difference between the "vault" and the "eye", Fujita suggested that the eye should be clearly distinguished from the vault since the former represents a small, circular column which stands semi-vertically and is surrounded by a vortex of high tangential wind velocity. Fujita (1958) estimated that the tangential velocity around the eye of the storm which produced the Illinois tornadoes of April 9, 1953 was about 40 kt at a distance of one mile from the center of the eye. A collection of four radar pictures of hook echoes appears in Fig. 3. These examples suggest that the vault is predominant in very early stages of the hook-echo development when the rotational rate of a thunderstorm cloud is relatively low. As the rotation becomes faster, an eye forms to the south or southeast end of the vault. Even though we have not obtained a good example of a radar picture showing a well-developed vortex around the eye, it would be natural to suspect that such a picture would appear as a miniature hurricane with several spiral echo bands surrounding an eye.

The evolution of a hook-echo circulation may be expressed as follows:

A. Initial Stage: A thunderstorm starts rotating slowly, forming a vault in the region where the updraft is the strongest. According to Browning's (1964) definition a vault may appear even before the onset of the storm's rotation as long as the updraft is sufficiently intense to result in inadequate time for droplet growth and to inhibit the reentry of large hydrometeors.

B. Development Stage: As the storm's rotational rate increases, the air converging toward the foot of the updraft can no longer reach the circulation center because the angular momentum, which must be transported inward without increasing the tangential velocity

enormously, is too large. Thus a small eye forms at the low level first and rapidly extends upward.

C. Mature Stage: In this stage the eye of the storm reaches almost to the top of the cloud, thus initiating upper divergence or significant outflow at the cloud-top level. Such a divergence aloft would efficiently inhibit the entry of hydrometeors into the eye from the cloud-top level. Near the ground, an intense inflow with strong tangential velocity creates a vertical column of rotating air surrounding the eye. The tangential velocity outside the circle of maximum wind would drop hyperbolically outward. The diameter of noticiable circulation will be about 30 miles.

D. Dissipating Stage: The diameter of the circulation reaches a maximum in this stage. The diameter then decreases as the maximum tangential wind speed decreases rapidly. Associated radar echoes would assume the shape of several spirals giving the impression that the storm is a miniature hurricane.

4. Location of Tornadoes in Relation to the Eye of the Tornado Cyclone

From a terminological point of view, if one emphasizes the geometric patterns of radar echoes the above-mentioned four stages would represent a complete evolution of a rotating thunderstorm. If we emphasize the circulation accompanying these storms, we may consider that the circulation increases through stages A and B, reaching a maximum in stage C, and finally disappears in stage D. The whole system may thus be called a mesocyclone initiated by a rotation of a thunderstorm. According to the definition by Brooks (1949), a mesocyclone accompanied by one or more tornadoes is called a tornado cyclone.

Surveys of tornadoes indicate that a family of tornadoes forming inside a tornado cyclone may form in one of three modes: the parallel mode, the combined mode, and the series mode. Based on the damage surveys of the Scottsbluff tornadoes by Van Tassel (1955), the Fargo tornadoes by Fujita (1960), the Dallas tornadoes by Hoecker (1958), the Worcester tornadoes by Penn et al. (1955), the Blackwell tornadoes by Staats and Turrentine (1956), the Illinois tornadoes by Fujita (1958), and Chapter II (SMRP Report No. 49), the positions of the tornadoes relative to the tornado-cyclone center are shown in Fig. 4. In this model of tornado paths,

formation of parallel-mode tornadoes takes place mostly on the right-hand side of the eye of a tornado cyclone, while those of the series mode occur near the center of the eye. Of interest is the change from the parallel mode to the series mode. Such a change has been found quite frequently. However, no case in which a series-mode family changed into a parallel-mode family has been found. This would imply that the structure of a tornado cyclone, which is favorable for the production of a parallel-mode family, somehow changes into that likely to produce a series mode. Further study has indicated that the parallel-mode family forms out of storms in stage B, the Development Stage, while the series-mode one forms out of storms in stage C, the Mature Stage. The reason for such a preference in tornado families is not known at the present time. We may suspect, however, that the concentration of vorticity around the center of a tornado cyclone takes place as the storm stage progresses from A to B to C. In stage C, the central region of a tornado cyclone seems to act like a weak tornado with a very large diameter. Periodic concentration of vorticity near the central region would produce a series-mode tornado.

5. Circulation Around Tornado J-4 Estimated from Tecumseh Wind Records

In order to study the 151-mph gust recorded at Tecumseh, Michigan in relation to tornado J-4, a 40-min section of the wind trace in Fig. 1 was enlarged. Figure 5 shows such an enlargement including wind velocities plotted at the bottom. Using heavy line segments, the successive maxima and minima were connected to show the range of the wind fluctuation clearly. The numbers next to the plotted winds represent the gust speed in knots. The highest gust of 151 mph occurred between 1907 and 1908 CST when the direction was shifting rapidly from WSW to WNW, suggesting that it was recorded when the tornado center was passing just to the north of the station.

Figure 6 was made to determine the wind field in relation to the damage area and radar hook echo J, which produced four tornadoes of the combined mode. Tornado J-4 was of the series mode. The upper chart in Fig. 6 indicates that the wind tower was located near the southern boundary of the damage path. It also shows that the diameter of the eye in the PPI echo was approximately the width of the damage path. This does not mean that the diameter of the tornado eye was over two miles; it could be considerably smaller. The lower chart shows the space cross-section of winds converted from the time cross-section of the Tecumseh winds. The wind

pattern seems to be affected by the cyclonic circulation of the tornado cyclone as well as by the tornado which was near the cyclone center.

Since tornado J-4 was one of the series of tornadoes belonging to a combined-mode family, we may reasonably assume that it moved with the center of the tornado cyclone at 60 mph toward the east-northeast. Due to the significantly low pressure around the tornado center, the surface wind field around the tornado axis represents a circular wind field superimposed upon a straight flow which represents the translational motion of the storm. Figure 7 shows the stream lines of relative flow and was obtained by subtracting the 60 mph straight flow from the winds recorded in Fig. 6. There are two important features in this figure. The first is that the tornado circulation appears only inside the dashed circle in the figure. The other is that outside this area the relative winds beneath the echo are more or less straight with increasing wind speed toward the tornado-cyclone center, which represents the tornado center in this case. It is, therefore, difficult to depict the flow accompanying the tornado cyclone by using the relative winds as shown in Fig. 7. The whirling wind around tornado J-4 is presented in Fig. 8 by enlarging a portion of Fig. 7. The dashed circle represents the boundary of the wind field of tornado J-4. Shown in the upper half of the dashed circle is the profile of the tangential wind speed plotted against the radii in the front and rear sectors of the storm. It shows that the tangential wind speed increases toward the center inversely proportional to the radius, implying that the eye or the core circulation of this tornado was surrounded by an irrotational vr vortex. The circulation of the vortex is estimated to be

$$\Gamma = 2\pi rv \cong 180\pi \text{ mi}^2\text{hr}^{-1}$$

If we assume that this circulation remains constant everywhere outside the core, the maximum wind at the core boundary would be

$$U_{max} = \frac{\Gamma}{2\pi r_{core}} \cong \frac{90}{r_{core}}$$

which is inversely proportional to the core radius. Tornado J-4 produced widely-scattered medium damage to the north of the wind tower. If we assume that the 3-mile wide damage path was caused by a tornado with a core of one mile in diameter, V_{max} would be about 180 mph. The maximum wind speed including the translational motion of the storm was, therefore, about 240 mph.

In fact, tornado K-3 also contributed to the overall damage path north of Tecumseh, although eyewitness accounts indicated that the first one caused most

of the damage. Figure 1 also shows that the maximum wind speed of K-3 was 85 mph which is slightly more than the translational velocity of the tornado.

6. Relative Surface Winds and Perturbed Winds Accompanied by Fast-Moving Tornadoes and Tornado Cyclones

It was shown in Figs. 7 and 8 that the wind velocity representing the vortex motion around a tornado axis near the surface can be obtained by subtracting from the total wind the translational velocity of the tornado center. In other words, the surface winds around a fast-moving tornado are very similar to those inside a rotating air column extending upward from near the surface.

A question which will arise immediately is what will be the diameter of such an air column inside which the tangential speed decreases outward. According to Fig. 8, the diameter seems to be about 5 miles. A relative wind of about 20-mph tangential speed is seen along the outermost boundary, indicated by a dashed circle. It seems that this rotating air column, 5 miles in diameter, is acting as an obstacle to the relative winds from the east-southeast. Right at the ground, where theoretically the air does not move even inside a tornado, the relative wind velocity should be opposite to that of the translational velocity of the tornado. A rotating air column such as shown in Fig. 8 must, therefore, be undercut by an extremely shallow layer. As the height above the ground increases from the order of inches to feet, the relative winds quickly change into those representing a column circulation around the center of a traveling tornado. This implies that the tornado inflow takes place inside a very shallow layer just above the ground.

Because of the fact that a tornado cyclone is accompanied by a much weaker wind system than that of a tornado, relative surface winds inside a tornado cyclone do not always represent a relative flow. Figure 7 showed that relative surface winds of a fast-moving tornado cyclone appear to blow through the region of the cyclone. Since the tornado cyclone, as well as most others, was located over a region where the southerly surface winds are about 30 mph, a moving tornado cyclone with a few-millibar pressure drop at the center is not strong enough to modify the 30-mph southerly wind or 55-mph relative wind from the east-southeast into a cyclonic flow within the area of the tornado cyclone.

Assuming, however, that a tornado cyclone induces perturbed winds no matter how fast it travels, the field of perturbed winds can be obtained by subtracting estimated

undisturbed winds from the total winds recorded by the Tecumseh wind recorder. Taking the time changes in the undisturbed wind into consideration, it was changed linearly from SSE 31 mph at 1850 CST to S 31 mph at 1925 CST. Figure 9 shows the field of perturbed wind resulting from tornado cyclone J as it was moving north of Tecumseh. A dashed circle in the figure represents the region of the whirlwind around the tornado center. Winds outside the circle form a spiral flow extending about 20 miles from the tornado-cyclone center.

It should be noted that the streamlines of perturbed winds are considerably asymmetric, suggesting that most of the inflow takes place in the front quadrant of the tornado cyclone. More quantitative aspects of such an asymmetry will be understood by refering to Fig. 10 in which the intensities of the circulation and the radial outflow are plotted as functions of the radius. These intensities are defined by $V_t r$ and $V_r r$ which can be integrated, respectively, as

$$\Gamma = \int_0^{2\pi} V_t r \, d\theta, \text{ circulation}$$

and

$$F = \int_0^{2\pi} V_t r \, d\theta, \text{ influx,}$$

where V_t, V_r, and θ denote tangential velocity, radial velocity, and the horizontal angle around the cyclone axis. The product of V and r, represents the circulation or outflow per unit angle around the cyclone axis, and its intensity, is a function of r and θ within the tornado cyclone.

Figure 10 indicates that the circulation intensity is negative or very small in the front quadrant some 20 miles away from the center. As the distance from the center decreases the intensity gradually increases to about 100 stat $mi^2 hr^{-1} rad^{-1}$. The intensity increase continues after the passage of the center, reaching a maximum in the rear quadrant about 15 miles from the center. We may postulate, therefore, that a certain time is required for the surface winds to acquire a cyclonic circulation when a tornado cyclone aloft moves over an area. In this specific case, about 40 min was required for the air parcel to travel from front to rear quadrant of the tornado cyclone.

The field of inflow intensity within this tornado cyclone was also quite asymmetric. In the front quadrant the inflow increased to a maximum about 15 miles from the center, but the inflow intensity was more or less constant outside a circle about 8 miles in diameter. The inflow intensity around this circle was about 150 stat $mi^2 hr^{-1} rad^{-1}$. If constant convergence inside this circle is assumed, the mean convergence

would be about 20 hr^{-1} or about 500×10^{-5} sec^{-1}. If the region of the tornado bounded by the dashed lines is excluded from the region of convergence by the tornado cyclone, a reduction of the convergence area would increase the convergence to about 800×10^{-5} sec^{-1}. Nevertheless, convergence of this order of magnitude would result in a 30 to 40 ft sec^{-1} updraft at the 5000-ft level.

The inflow in the rear quadrant is extremely small. This characteristic coincides with the fact that usually few or no spiral rain echoes are observed in the rear quadrant of tornado cyclones. Figure 3 includes two good examples of this feature; namely, April 11, 1965, and April 9, 1953, which were cases accompanied by well-developed tornado-cyclone circulations. Note that two spiral echoes with crossing angles of more than 40 deg are seen in both examples.

7. The Nature of Characteristic Cycloidal Marks on the Ground

Since Van Tassel (1955) first reported on the elliptic marks left on fields by the North Platte Valley tornado of June 27, 1955, several other such phenomena have been reported. Prosser found a large number of cycloidal marks in a series of vertical aerial pictures photographed along the path of a Nebraska tornado of May 5, 1964. The aerial survey of the Palm Sunday tornadoes of April 11, 1965 as reported in Chapter II (SMRP Research Paper No. 49) revealed the existence of a large number of well-defined cycloidal marks in Indiana and Ohio.

Complete interpretations of these marks have not been made at the present time; however, both Van Tassel and Prosser concluded that they are closely related to the rotational and translational motions of each tornado. To determine the estimated tangential wind speed, Van Tassel assumed that the marks were produced by something being carried with the speed of the revolving wind within the tornado funnel. Using C, the circumference of the ellipse; N, the number of scratch rings per mile; and S, the translational speed of the tornado as input data, he estimated a tangential wind speed of 484 mph. Prosser considered, on the other hand, that these marks on the photographs are probably the result of light reflected differently from the disturbed and the undistrubed areas. This was based upon his closer inspection of high-resolution aerial photographs and also upon a damage survey by R. E. Meyers, State Climatologist for Nebraska, who stated "the path gave the impression that an enormous vacuum cleaner had swept the ground clean of vegetation, loose soil, all other movable objects." Careful examination of the aerial photographs by Prosser

led him to make an important suggestion that the vortex diameter was oscillating about the mean since the radius of curvature of closed loops varied along the tornado path.

In an attempt to find out the nature of these marks from the Palm Sunday case, the author took a number of 35-mm telephoto pictures from a low-flying Cessna-310. Figure 11, reveals the detailed structure of the marks, the overall view of which appears in Fig. 39, Chapter II. A cycloidal line superimposed upon the telephoto picture was drawn by following smoothly one of the most pronounced lines in the picture. As can be seen there are a few more cycloidal marks within the one cycle of the cycloid in the figure, suggesting strongly that several "spots" rotating around the tornado center were responsible for producing these cycloidal marks. If we assume, like Prosser did, that these spots represent areas of very strong suction capable of vacuum cleaning the soil on a plowed field, it is feasible to determine the size and position of these spots relative to the tornado center.

Closer inspection of a number of telephoto pictures and repeated visual observation from an altitude of 500 feet led the author to believe that the cycloidal lines in Indiana and Ohio caused by the Palm Sunday tornadoes were not the loosened or blown-off soil from plowed fields. Due to the early date of the Palm Sunday tornadoes, it is not likely that the fields had been recently plowed as was the case of the Scottsbluff, Nebraska tornadoes. The Nebraska tornado studied by Prosser occurred on May 5 when some fields could have been plowed prior to the occurrence of the tornado.

It is of interest to note that Prosser feels that the marks are the result of differential soil characteristics, while the author thinks that they represent narrow bands of debris accumulation. Nonetheless, both researchers agree that they represent loci spots which act like nature's vacuum cleaners. In Prosser's case, the vacuum cleaner was so strong that it loosened up and vacuum cleaned the soil and vegetation. The debris accumulation seen in the author's case can be explained as the result of vacuum cleaners which are strong enough to converge debris, but not capable of sucking up the accumulated debris, which will remain within a layer a few inches deep above the ground. However, in order to determine the characteristics of tornadoes just above the surface, it is necessary to examine the marks observed in aerial pictures by means of detailed ground survey.

To give an idea of the amount of suction that might be present in a tornado, for example, it may be calculated that a household vacuum cleaner head with 15 ft sec^{-1}

suction speed will produce a convergence of

$$\text{Conv.} = \frac{\text{suction speed}}{\text{height of head above the floor}} = 100 \text{ sec}^{-1}$$

when the head was placed about 2 inches above the floor. If we assume that a convergence of 10 sec^{-1}, only one-tenth of that of household vacuum cleaner exist near the ground, it would result in vertical motions of 5 ft sec^{-1} at 6 inches above the ground, 10 ft sec^{-1} at one foot, 100 ft sec^{-1} at 10 ft, etc.

Despite the fact that we do not know the exact magnitude of the convergence giving rise to the formation of these ground marks, it is obvious that they can be produced only if the convergence near a tornado center is concentrated at several spots which rotate around the center. In case the convergence takes place uniformly around a circular area, a uniform damage belt such as that produced by a rotating grinder would be expected.

The size of these spots with strong convergence, as determined from the width of cycloidal lines is only several to 20 ft, implying that the convergence inside a tornado is concentrated at several spots which rotate around the traveling tornado center. Such spots of concentrated convergence may be called the "suction spots," and the ground marks appearing along the loci of suction spots, the "suction marks." Suction marks, if preserved, would represent a group of cycloidal curves; however due to strong winds on the rear side of a traveling tornado, the marks produced by suction spots while moving on the front side are either partially or totally destroyed by those suction spots in the rear side. This is why in aerial pictures we frequently see the rear half of the cycloidal marks more distinctly. Before the end of the tornado wind, the rear half will be swept by the remainder of the whirlwind. The "drift marks" as indicated in Fig. 11 are the common features produced by debris which is blown off in the direction of the final strong winds.

8. Shape of Cycloidal Marks, their Loop Width and Loop Shift

If a suction spot is assumed to rotate around the tornado center at a constant radius, the locus of the spot can easily be computed as a function of U, V, and R which are, respectively, the translational speed, tangential speed, and radius between the spot and the tornado center. Parametric equations of a cycloid with the x-axis taken along the path of a tornado center are

$$y = R \sin \omega t$$
$$\text{and} \quad x = Ut + R \cos \omega t \qquad (1)$$

where ω denotes the angular velocity of a suction spot and t, the time measured from the initial x-axis crossing of the spot. If $c = \omega t/2\pi$, the total rotation number of a suction spot around the tornado center, is substituted in Eq. (1), and, if the resulting equation is differentiated in order to obtain the slope, then

$$\frac{dy}{dx} = \frac{dy/dt}{dx/dt} = \frac{V\cos 2\pi c}{U - V\sin 2\pi c}$$

$$= \frac{n\cos 2\pi c}{1 - n\sin 2\pi c} \quad , \tag{2}$$

where $n = V/U$, the ratio of the tangential and the translational speeds. Eq. (2) indicates that the slope of the cycloidal curve is a function of both n and c without depending upon R, the distance of the suction spot from the rotation center. This means that the overall shape of a cycloidal mark depends only upon n, the ratio of tangential and translational speeds.

Figure 12 was made by changing n from 1.0 to 10. The height of the loop as well as the loop width increases with n, becoming very close to $2R$ when n exceeds 10.

The loop width is measured as the difference of x when the slope changes from plus infinity to minus infinity, which occurs when

$$1 - n\sin 2\pi c = 0$$

$$\text{or} \quad 2\pi c = \sin^{-1}\frac{1}{n} \quad . \tag{3}$$

The time corresponding to this rotation angle is

$$t = \frac{2\pi c}{\omega} = \frac{2\pi cR}{V}$$

which is now put into Eq. (1) to obtain

$$x_1 = \frac{2\pi cR}{n} + \frac{R\sqrt{n^2-1}}{n}$$

$$\text{and} \quad x_2 = \frac{(\pi - 2\pi c)R}{n} - \frac{R\sqrt{n^2-1}}{n} \quad .$$

Thus we have

$$w = x_1 - x_2 = \frac{R}{n}\left\{2\sqrt{n^2-1} - \pi + 2\sin^{-1}\frac{1}{n}\right\} \tag{4}$$

where w denotes the width of the loop which naturally increases with n.

In order to define a non-dimensional quantity related to the loop width, we

introduce the ratio of w and 2R , thus

$$W = w/2R = n^{-1}\left(\sqrt{n^2-1} - \frac{\pi}{2} + \sin^{-1} n^{-1}\right) \qquad (5)$$

which may be called the "relative loop width." It is evident that this quantity varies as the function only of n. It is, therefore, feasible to determine n from measured values of W. Figure 13 presents the variation of n as a function of W. This figure permits us to determine V from a suction mark on an aerial photograph and the known value of U.

When a large number of suction marks appear, such as in the schematic pattern in Fig. 13, it is very difficult to identify the loops produced by a single suction spot which rotated more than once around the tornado center. In such a case, the distance of the loop shift, s can be estimated from W and R. We shall now define the non-dimensional quantity S as

$$S = s/2R = \frac{2\pi R}{n}/2R = \frac{\pi}{n} \quad , \qquad (6)$$

which may be called the "relative loop shift." Since n and W are functions of each other, we are able to express S as a function of W only. The right-hand diagram in Fig. 13 presents the relative loop shift as a function of W. It is evident that S decreases from a maximum value of π to zero as the relative loop width increases to 1.0.

More accurate values of n and S are given in Tables I and II in which both quantities are computed by increasing W at 0.01 intervals. The tables permit us to obtain n between 1.00 (when W = 0.00) and 38.95 (when W = 0.96). Such a range would be sufficient for analytical purposes, since there will be no tornado when n is less than 1.0, and since cycloidal marks are too close to each other if W exceeds about 0.9.

Table I. Relative loop width, W, in increments of 0.01, vs. n, the ratio of tangential to translational speeds.

	0.00	0.01	0.02	0.03	0.04	0.05	0.06	0.07	0.08	0.09
0.0	1.00	1.05	1.08	1.11	1.14	1.16	1.19	1.21	1.24	1.26
0.1	1.29	1.31	1.33	1.36	1.38	1.41	1.44	1.46	1.49	1.51
0.2	1.54	1.57	1.60	1.63	1.66	1.69	1.72	1.75	1.78	1.81
0.3	1.85	1.88	1.92	1.95	1.99	2.03	2.07	2.11	2.15	2.19
0.4	2.24	2.29	2.33	2.38	2.43	2.48	2.54	2.60	2.65	2.71
0.5	2.78	2.84	2.91	2.98	3.06	3.13	3.21	3.30	3.39	3.48
0.6	3.58	3.68	3.78	3.90	4.02	4.14	4.27	4.42	4.57	4.72
0.7	4.89	5.08	5.27	5.48	5.70	5.95	6.21	6.49	6.81	7.15
0.8	7.52	7.94	8.40	8.91	9.49	10.14	10.89	11.76	12.76	13.95
0.9	15.38	17.13	19.31	22.12	25.86	31.09	38.95	***	***	***

*** No values computed because of too large n.

Table II. Relative loop width, W, in increments of 0.01, vs. S, the relative loop shift.

	0.00	0.01	0.02	0.03	0.04	0.05	0.06	0.07	0.08	0.09
0.0	3.14	2.97	2.90	2.83	2.76	2.70	2.64	2.59	2.54	2.49
0.1	2.44	2.40	2.36	2.31	2.27	2.23	2.18	2.15	2.12	2.08
0.2	2.04	2.00	1.97	1.94	1.90	1.87	1.84	1.80	1.76	1.73
0.3	1.70	1.67	1.64	1.60	1.57	1.54	1.52	1.49	1.46	1.43
0.4	1.40	1.37	1.35	1.32	1.29	1.26	1.24	1.21	1.18	1.16
0.5	1.13	1.10	1.08	1.05	1.02	1.00	0.98	0.95	0.93	0.90
0.6	0.88	0.85	0.83	0.81	0.78	0.76	0.73	0.71	0.69	0.66
0.7	0.64	0.62	0.60	0.58	0.55	0.52	0.50	0.48	0.46	0.44
0.8	0.42	0.40	0.38	0.35	0.33	0.31	0.29	0.27	0.25	0.22
0.9	0.20	0.18	0.16	0.14	0.12	0.10	0.08	0.06	0.04	0.02

9. Computation of the Rotational Rate of Suction Spots

It has been shown in the previous section that n, the ratio of tangential and translational speeds of a suction spot can be obtained by measuring W, the relative loop width on an aerial photograph. Under the fair assumption that a suction spot rotates around the tornado center, we obtain the tangential speed of a suction spot as a product of n and U_{TOR}, the translational speed of the tornado.

The speed of a fast-moving tornado seems to be rather constant, probably because tornadoes tend to move, on the average, with the speed of the parent thunderstorm. Figure 14 is a time-space diagram of a family of six tornadoes in series mode which traveled from Indiana to Ohio as shown in Fig. 2, Chapter II. This family of tornadoes left a damage path in an almost straight line 274 miles long during a period of 4 hr 23 min. From the slope of a diagonal line through the black dots in the figure, U_{TOR} was estimated to be 62.5 mph.

In order to apply the technique of cycloidal curve analysis presented in the previous section, a picture of a group of suction marks taken along the path of the above-mentioned tornado family was investigated in detail. An aerial photograph taken and rectified by the author is shown in Fig. 15. The horizontal scale and the estimated path of the tornado center are superimposed on the photograph.

Traced suction marks appearing in Fig. 16 permit us to compute the relative loop width, W, which can be converted into both n and S by using the two curves in Fig. 13. In this case, we computed S to represent the distance of the loop shift. Two persistent suction spots, identified with letters a and e, were followed, respectively, during one and four rotation periods, to determine locations of their periodic appearances.

The open circles with number 1 through 7 are the estimated positions of the tornado center after the suction marks completed each revolution around the center. The distance of travel during each revolution can be converted into the rotational period by assuming U_{TOR}= 62.5 mph. The periods in seconds given in the figure are the rotational periods thus obtained.

The figure also shows the positions of the suction spots when the tornado center was at the locations 1 through 7. In determining the positions of these suction spots, the radius vectors were obtained by measuring the distance between the loop tops and the path of the tornado center. The phase angles were computed from the positions of the bases of perpendiculars dropped from each loop top to the path of the tornado center.

Of interest is the change in the stippled area obtained by connecting the suction spots smoothly. The number of suction spots varied between 4 and 5 while their radius vectors changed considerably from time to time. It should be noted that the rotational period decreased as the mean diameter of the stippled area shrunk with the eastward movement of the storm. This would imply that (1) the shrinkage of the stippled area increased the rotational rate, keeping probably the angular momentum constant and that (2) the stippled area represents the central core of the tornado, which kept deforming rather rapidly.

The mean tangential speeds of the suction spots when the tornado center was at locations 1 through 7 are 110, 114, 111, 118, 118, 111, and 104 mph, respectively. By adding 62.5 mph to these values, we obtain the maximum ground speeds of 172, 176, 173, 180, 180, 173, and 166 mph, respectively.

These tangential speeds are very similar to those of funnel rotation obtained by Fujita (1959) using motion pictures of the Fargo tornadoes of June 20, 1957. The tangential speeds of seven pendants appearing at the base of a sheared-off funnel just above the ground were 112 (90), 112 (60), 93 (30), 100 (60), 111 (110), 100 (100), and 102 mph (90), respectively. The numbers in parenthesis are the distance in meters of the pendants from the funnel center.

From these results, it will be reasonable to assume that these suction spots rotate around the tornado center with approximately the rotational rate of the funnel.

10. Conclusions

Through the study of the wind speed of the Palm Sunday tornadoes, five important characteristics of tornado circulation were found. They are: (1) a tornado circulation is characterized by a nearly circular core surrounded by an irrotational vortex, (2) there are several spots of strong suction along the edge of the core, (3) the core changes its shape and diameter, (4) the rotational rate of the core increases as the mean core diameter decreases, and (5) a tornado cyclone surrounding a tornado is almost axially symmetric as far as the pressure field is concerned, but the front and the rear sides are dominated by convergence and circulation, respectively.

This study has shown that it is highly important to perform aerial surveys of the damage paths of future tornadoes. Such surveys should investigate the damage patterns by undisturbed tornado vortices, such as could be formed over open fields.

REFERENCES

Brooks, E. M., 1949: The Tornado Cyclone. Weatherwise, 2, 32-33.

Browning, K. A., 1964: Airflow and Precipitation Trajectories within Severe Local Storms which Travel to the Right of the Winds. J. Atmos. Sci., 21, 634-639.

_____, 1965: Comments on "Formation and Steering Mechanisms of Tornado Cyclones and Associated Hook Echoes." Mon. Wea. Rev., 93, 639-640.

Fujita, T., 1958: Mesoanalysis of the Illinois Tornadoes of 9 April 1953. J. Meteor., 15, 288-296.

_____, 1960: A Detailed Analysis of the Fargo Tornadoes of June 20, 1957. Res. Paper No. 42, U.S. Dept. of Commerce, Weather Bureau, Washington, D.C., 67 pp.

_____, 1965: Reply to Comments on "Formation and Steering Mechanisms of Tornado Cyclones and Associated Hook Echoes." Mon. Wea. Rev., 93, 640-643.

Hoecker, W. H. Jr., 1958: The Dimensional and Rotational Characteristics of the Tornadoes and their Cloud System. The Tornadoes of Dallas, Texas, April 2, 1957. Res. Paper No. 41, U.S. Dept. of Commerce, Weather Bureau, 53-113.

Penn, S. et. al., 1955: The Squall Line and Massachusetts Tornadoes of June 9, 1953. Bull. Amer. Meteor. Soc., 36, 109-122.

Prosser, N. E., 1964: Aerial Photographs of a Tornado Path in Nebraska, May 5, 1964. Mon. Wea. Rev., 92, 593-598.

Staats, W. F., and C. M. Turrentine, 1956: Some Observations and Radar Pictures of the Blackwell and Udall Tornadoes of May 25, 1955. Bull. Amer. Meteor. Soc., 37, 495-505.

Van Tassel, E. L., 1955: The North Platte Valley Tornado Outbreak of June 27, 1955. Mon. Wea. Rev., 83, 255-264.

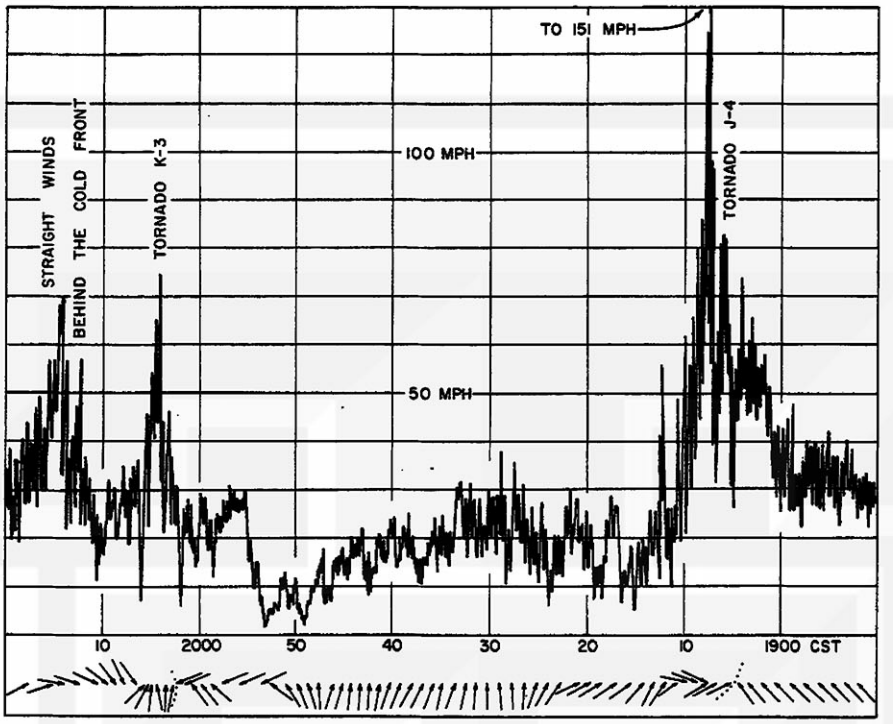

Figure 1. Wind recorder trace from Tecumseh, Michigan, on 11 April 1965, when two tornadoes passed north of the station. The recorder pen went off the chart at 151 mph. A combination of wind direction and wind speed indicates that the peak gusts at 1908 and 2004 CST were caused by two tornadoes, and the one at 2014 CST by straight winds associated with the passage of the cold front. (Courtesy of the Tecumseh Community Health Study, the University of Michigan).

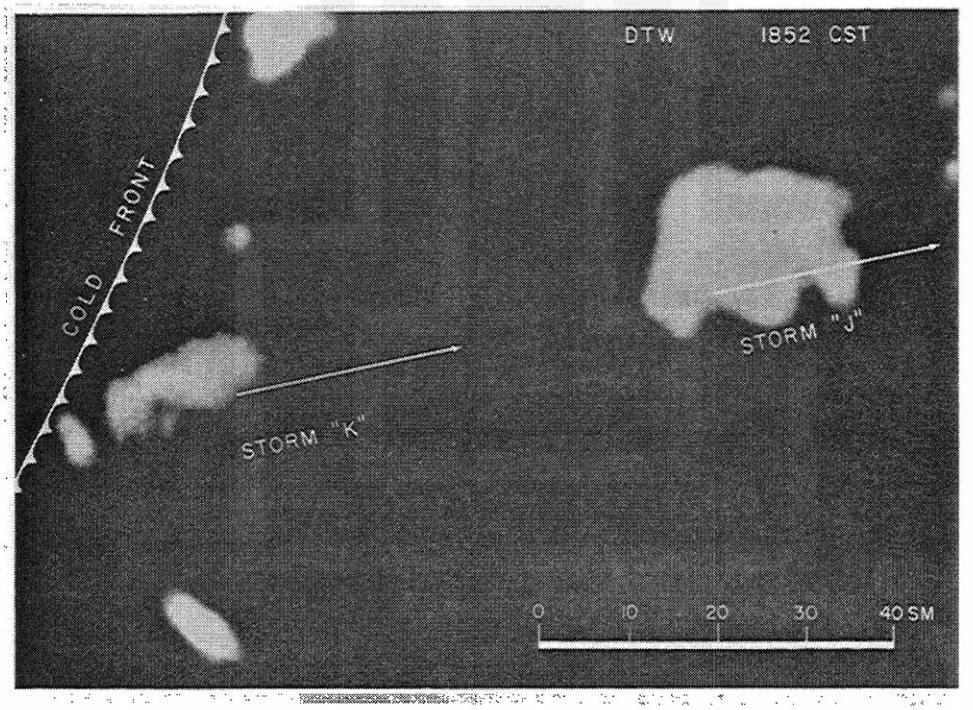

Figure 2. A WSR-57 radar picture from Detroit taken at 1852 CST with the cold front superimposed. Comparison of this picture with Fig. 1 shows the relationship between the peak gusts and the weather systems which produced them.

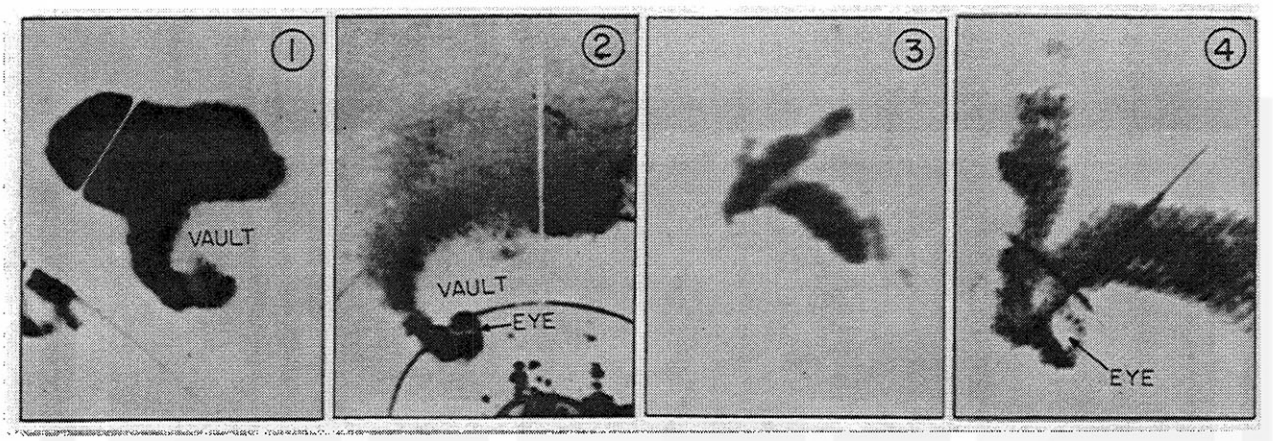

Figure 3. Four radar pictures showing stages in the intensification of tornado-cyclone circulation. Note that the first picture, a tornadic storm south of Chicago on 22 July 1963, shows a pendant finger attached to a large echo to the north. The circulation intensity appears to increase from picture 2 through picture 4 which represent the northeast Kansas tornadoes of 19 May 1960, the Palm Sunday tornadoes of 11 April 1965, and the Illinois tornadoes of 9 April 1953, respectively.

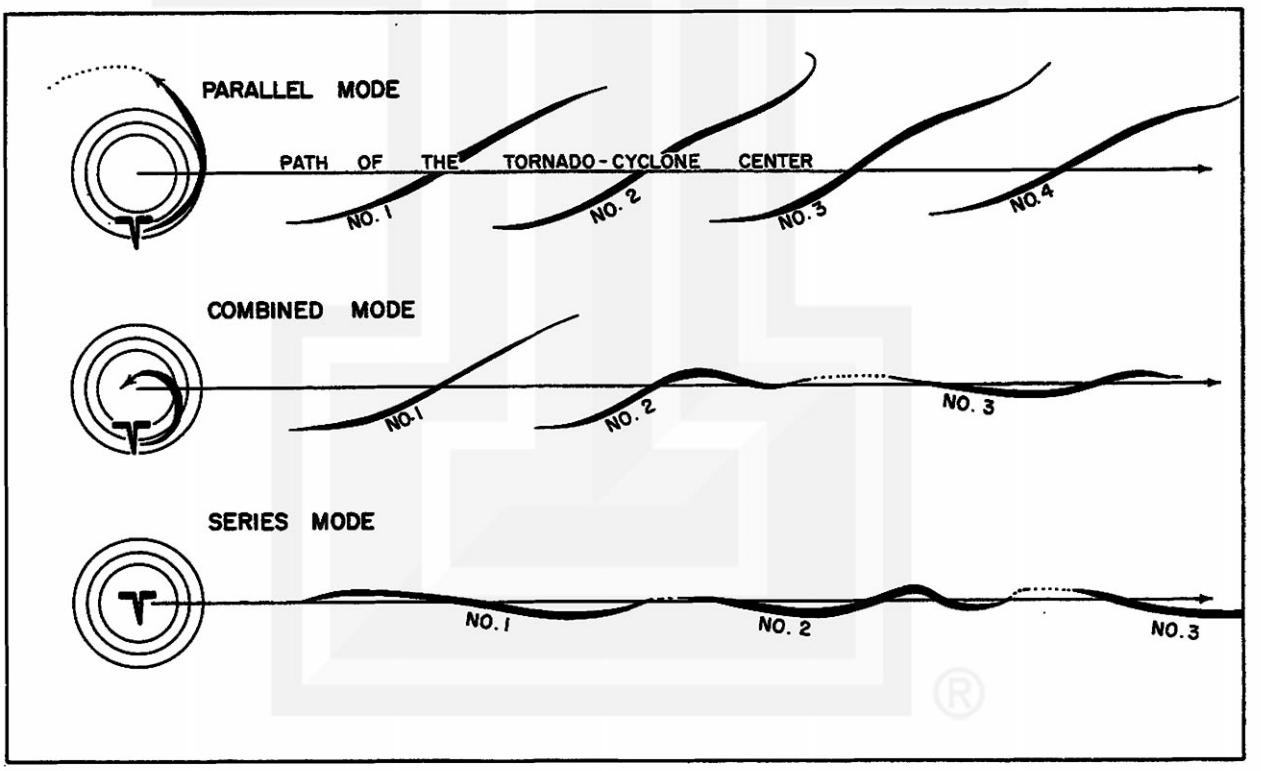

Figure 4. Three modes of damage paths produced by a family of tornadoes, namely; parallel, combined, and series modes.

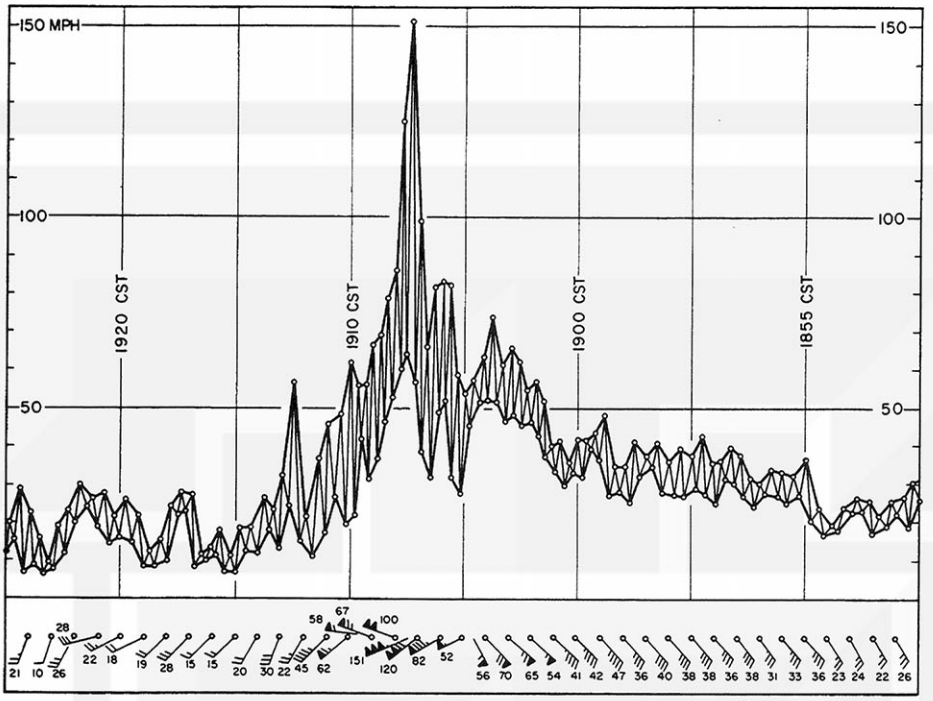

Figure 5. Enlargement of the wind recorder trace appearing in Fig. 1. In completing the wind speed chart, both time and speed of all visible maximum and minimum values were read from the recorded trace and then connected with straight lines. At the same time, successive maximum and minimum values were separately joined to show the range in the variation of gusty winds. Wind velocities plotted at the bottom represent 1-min means of maximum values in mph.

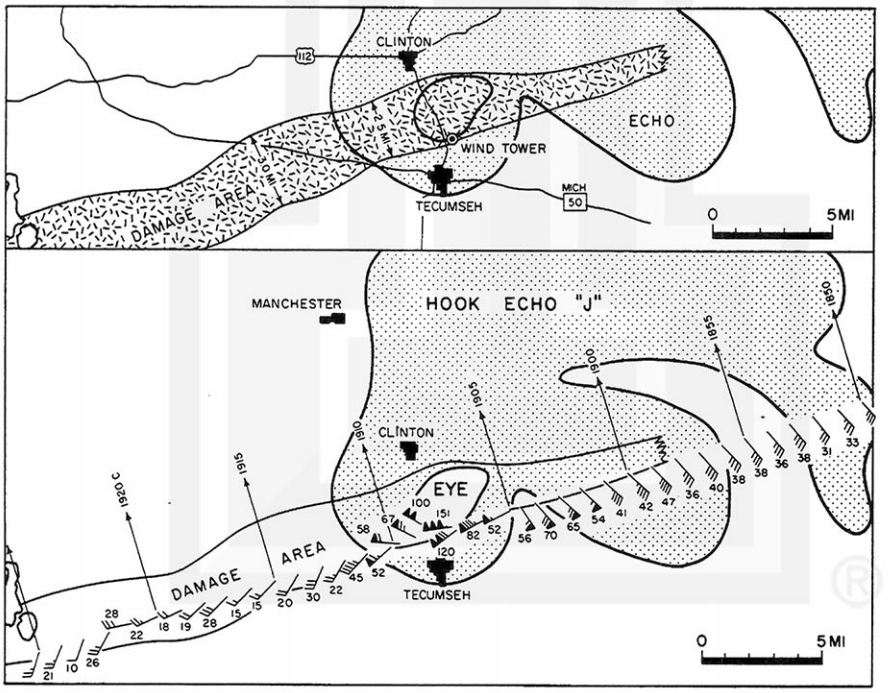

Figure 6. Damage area in relation to the hook echo at the time of the highest recorded wind (upper chart), and to the space section of the mean maximum winds (lower chart).

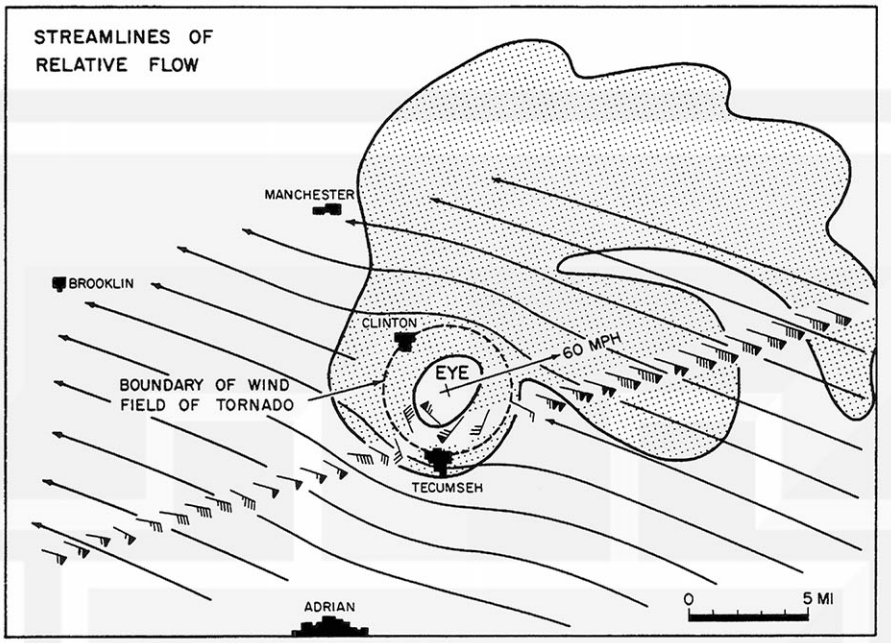

Figure 7. The space section of relative winds obtained by subtracting 60 mph, the translational velocity of the storm, from the 1-min means of maximum winds. Due to the rapid motion of the tornado cyclone, the relative winds computed tend to blow through the tornado cyclone near the ground. Inside the tornado area, as indicated by the dashed circle, the relative winds are circulating around the tornado center.

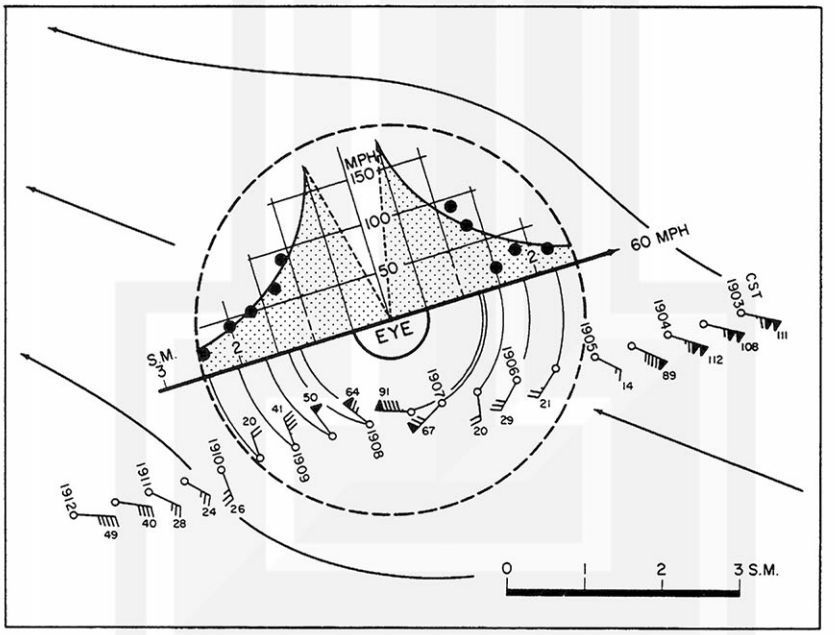

Figure 8. Enlargement of the field of relative winds inside the dashed circle shown in Fig. 7. This shows that an area within a circle of 5 mi in diameter was characterized by a tangential wind speed inversely proportional to the radius. The expected region of the eye of the tornado is indicated by the fine dashed line.

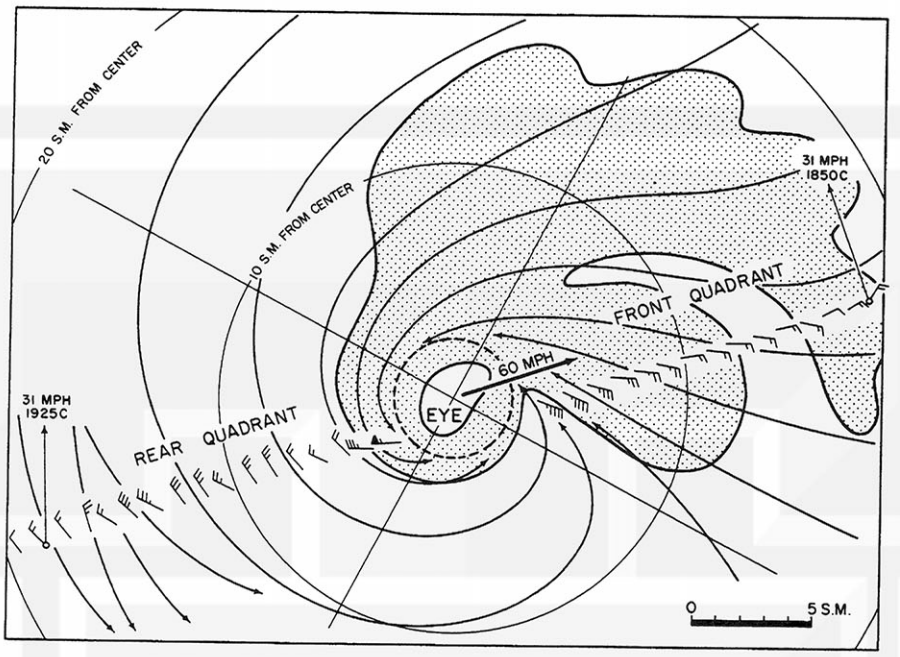

Figure 9. Perturbed wind field accompanied by the tornado cyclone in Fig. 1. Note that this wind field shows a definite sign of circulation and convergence, since this part of the wind field represents the vector difference between the actual wind and the undisturbed wind, computed by assuming that there was no tornado cyclone.

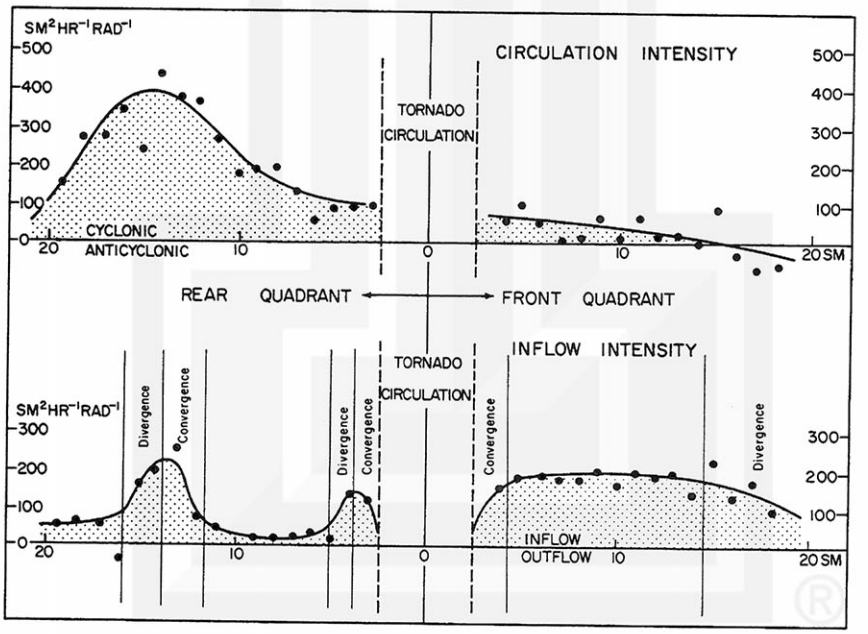

Figure 10. Radial distribution of circulation intensity inside the front and rear quadrant of the tornado cyclone. These intensities were computed from the perturbed winds as a function of the distance from the storm center.

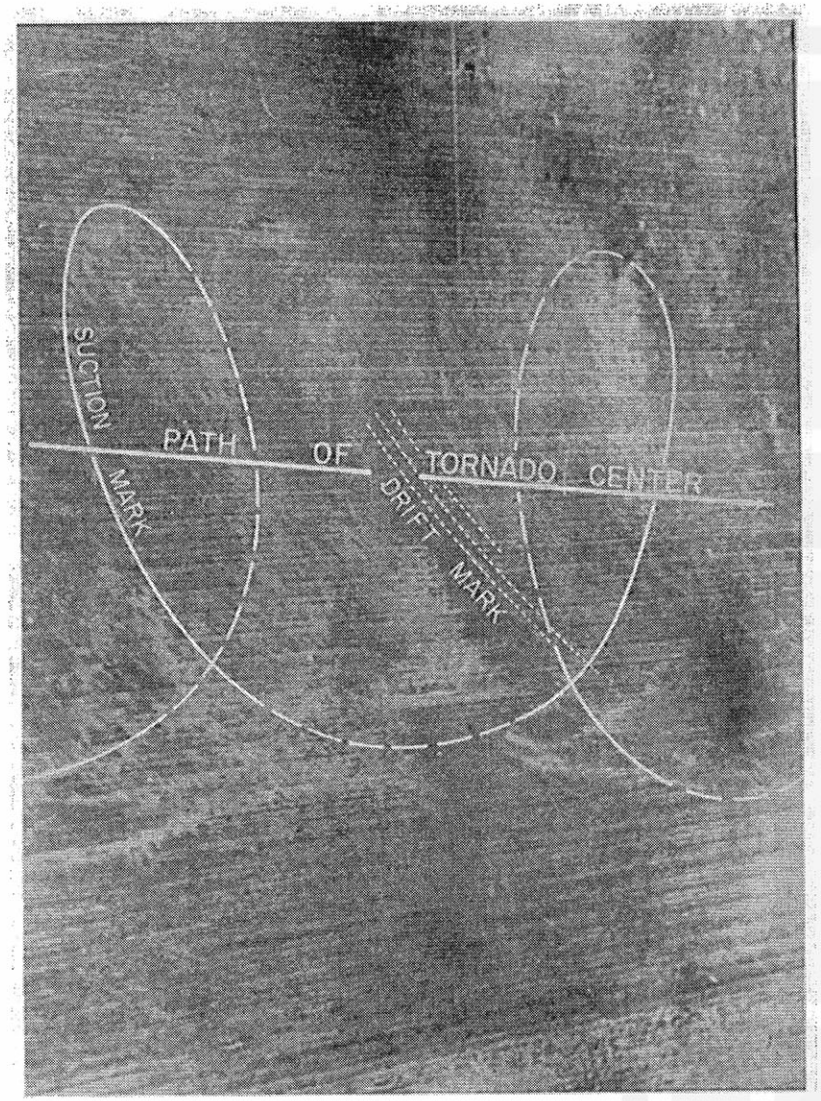

Figure 12. Theoretical cycloidal suction marks obtained by increasing the ratio of tengential velocity, V, to translational velocity, U, from 1.0 to 10.0. Note that the size of the loops increases as the tangential speed increases.

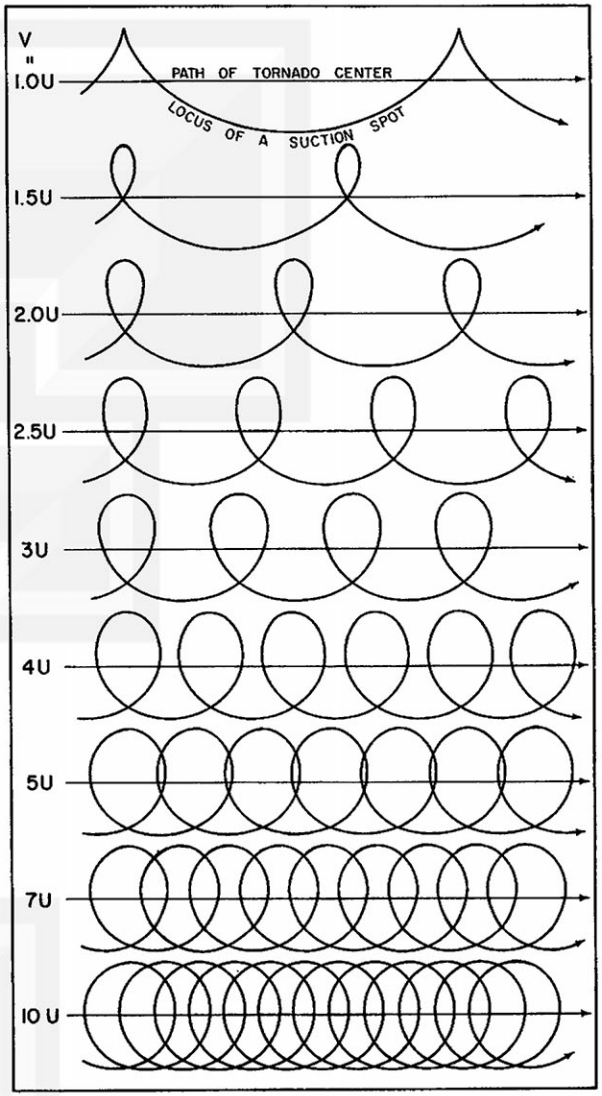

Figure 11. An aerial photograph of typical suction and drift marks left by a tornado on an unplowed field. This picture was taken with a 135-mm telephoto lens while flying over the area shown in Fig. 13, Chapter II (SMRP Research Paper No. 49).

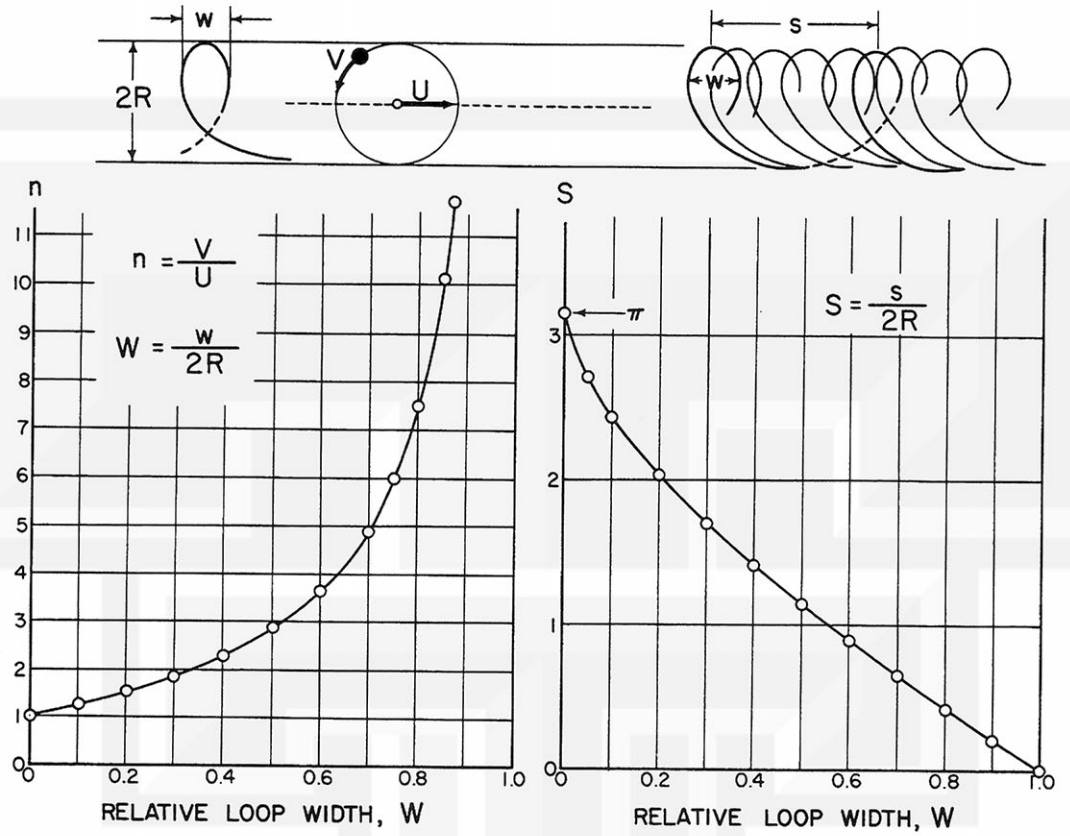

Figure 13. Variation of n, the ratio between tangential and translational speeds, and S, the relative shift, as functions of relative loop width, W, which can be measured on a rectified aerial photograph showing suction marks. This figure is used in determining both n and S from aerial photographs.

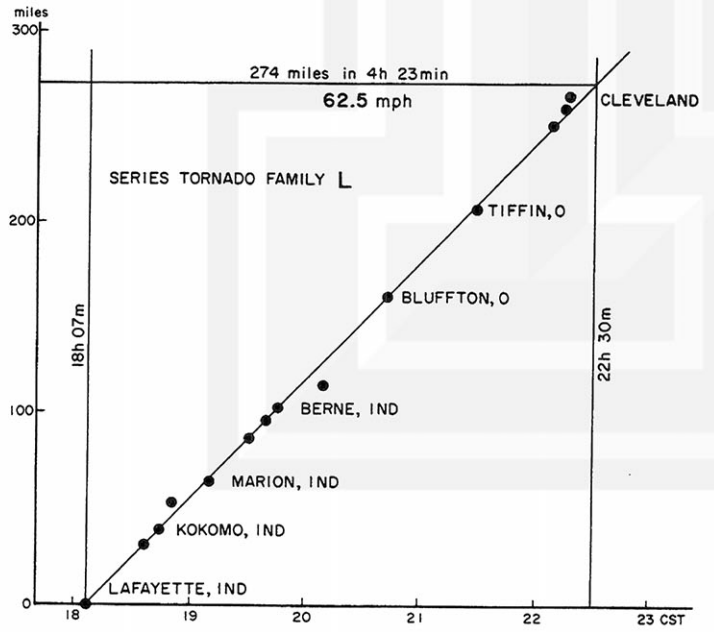

Figure 14. An x-t diagram showing the time and locations of Family L tornadoes in Indiana and Ohio. Refer to Fig. 2, Chapter II (SMRP Research Paper No. 49) for a more detailed picture.

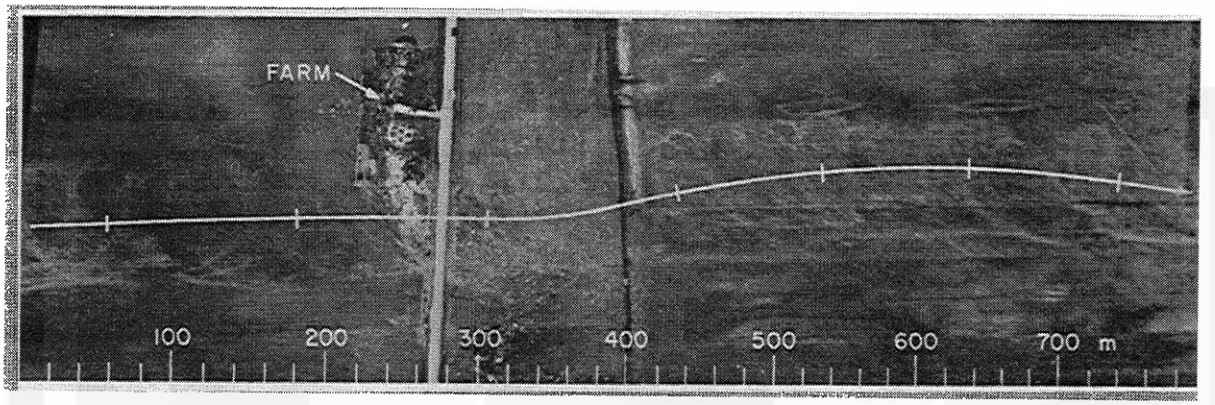

Figure 15. A rectified aerial photograph showing a large number of cycloidal suction marks. Refer to Fig. 39, Chapter II (SMRP Research Paper No. 49) for the original photograph.

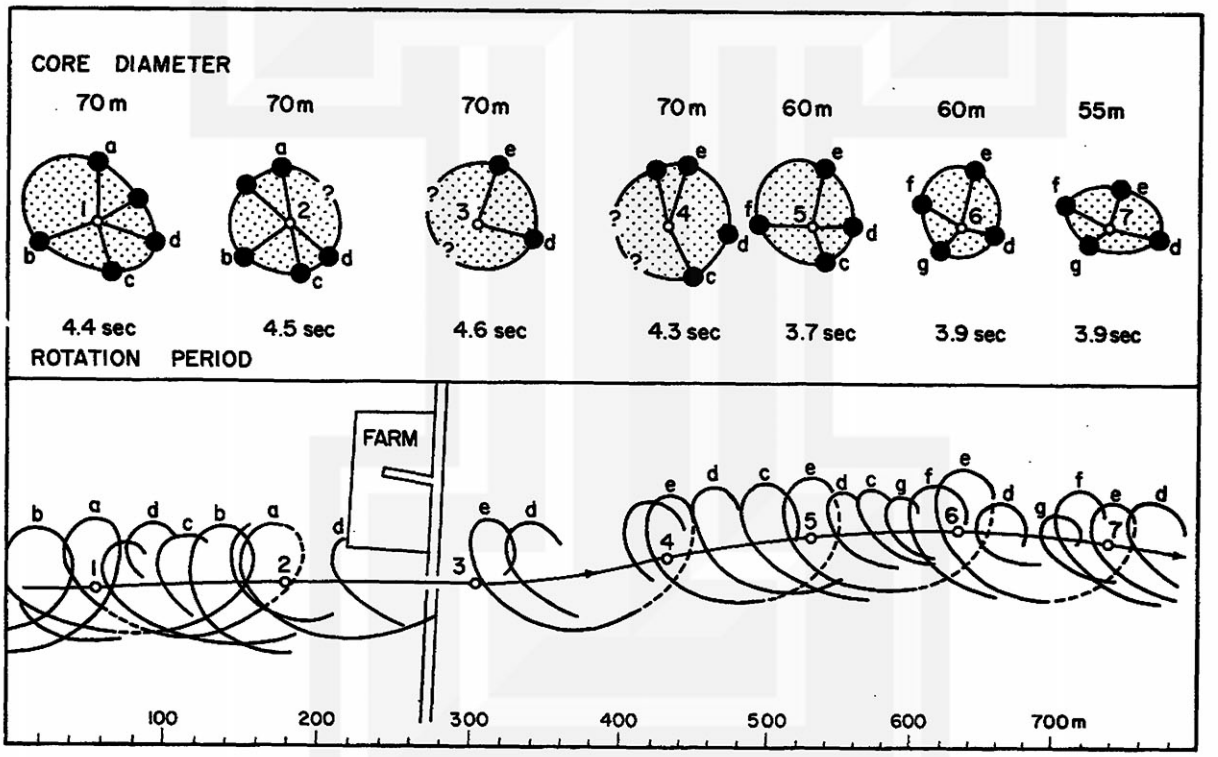

Figure 16. Change in the shape of the tornado core as determined from the analysis of the cycloidal suction marks shown in Fig. 15 (lower part). Core diameter, rotation periods, and funnel positions 1 through 7 are given in the upper part. It should be noted that the rotational rate increased as the core diameter decreased, suggesting a conservation of angular momentum.